Zorn, E.U., et al., 2023, Interactions of magmatic intrusions with the multiyear flank instability at Anak Krakatau volcano, Indonesia: Insights from InSAR and analogue modeling: Geology, https://doi.org/10.1130/G50693.1

# Supplementary material

# Interactions of magmatic intrusions with the multi-year flank instability of Anak Krakatau volcano, Indonesia: Insights from InSAR and analogue modelling

**Edgar U. Zorn*[1], Magdalena Vassileva[1], Thomas R. Walter[1], Herlan Darmawan[2], Leonie Röhler[1], Falk Amelung[3]**

[1]*German Research Centre for Geosciences GFZ, Telegrafenberg, 14473 Potsdam, Germany*

[2]*Geophysics Study Program, Department of Physics, Faculty of Mathematics and Natural Sciences, Universitas Gadjah Mada, 55281, Yogyakarta, Indonesia*

[3]*Department of Marine Geosciences, Rosenstiel School of Marine and Atmospheric Sciences, University of Miami, 4600 Rickenbacker Causeway, Miami, FL 33149, USA*

## SUPPLEMENT A: SENTINEL-1 FLANK DISPLACEMENT MONITORING BY INSAR

### Processing Methods:

We measured the displacement flank evolution using multi-temporal InSAR technique and exploited the Sentinel-1 data in both ascending (orbit 171) and descending (orbit 47) acquisition orbit in the period between 08th Oct 2014 and 19th Dec 2018. We adopted the Small BAseline (SB) method as implemented in the ENVI SARscape® software, using standard processing methods (Berardino et al., 2002). SB allows for a maximisation of the spatial and temporal coherence, and therefore maximises the displacement measurements over the flank, owing to the combination of interferograms with small normal and temporal baselines. We generate interferograms connecting each image with two previous and two following acquisitions. The original data has been multi-looked resulting in a pixel size of 15 m. We used the 30m resolution Shuttle Radar Topography Mission (SRTM) digital elevation model (DEM) via the Earth

Resources Observation And Science (EROS) Center 2017 to remove the topographic component from the interferograms and we filter the results using Goldstein filter (Goldstein and Werner, 1998) with tile sizes of 18px×18px. Finally we unwrap the interferograms masking out coherence lower than 0.2 and applying two-dimensional phase unwrapping algorithm Snaphu and we refer to the displacement measurement using a reference point located on the most northern part of the island considered stable (Fig. 2A). The results are displacement maps in ascending and descending line-of-sight (LOS). We further combined these two geometries using the incidence angle (e.g. Yun et al., 2006; Pepe and Calò, 2017) and derived vertical and horizontal components of displacement (Fig. 2A-F and S1D-F). Due to a significant increase in eruptive activity of Anak Krakatau beginning towards the end of May 2018, coherence was significantly reduced on the SW-flank and many unwrapped points became unreliable and had to be filtered out. To capitalise on the previously better coverage, we split our analyses into two separate datasets, one for interpreting data before the 29th May 2018, containing more reliable points on the SW-flank, and one dataset with fewer points used to interpret activity after.

**InSAR Limitations:**

While ground deformation signals extracted by InSAR are generally considered to be highly accurate, some limitations arise in the interpretation due to the relatively small size of the Anak Krakatau island (approx. 2 km in diameter) considering the ~15m resolution provided by Sentinel-1 SAR data. Consequently, the deformation signals are very localised, making the interpretation of fringes challenging, especially in the area of the active cone where frequent eruptions cause low coherence. The SB approach largely omits this problem by maximising the coherence, however, between single interferograms some fringes may become disconnected in low coherence areas and result in erroneous unwrapping. This happened in the ascending track in Oct 2018 (marked as an artefact, Fig. 1C), coinciding with a particularly strong eruptive phase with major surface changes and resulting minimal coherence. However, for our results, this problem is likely not a major issue as no further artefacts were found and the measured deformation rates are consistent through time. Another issue arising from the small island size is the choice of a stable reference point, which we placed in the northern part of the island (Fig. 2A). While the measured décollement slip did not affect this part of the island, suggesting this point to be a good reference, this is not as clear for the short -term intrusion events. The intrusions did cause notable uplift around the main cone (Fig.

2C, E), possibly affecting the reference point, so it is likely that some displacements and deformation rates are not as accurate during these instances. A further characterisation is not possible as the island is too small to pick other and more reliable reference points and the neighbouring islands Rakata, Lang, and Verlaten are vegetated and thus non-coherent. However, from the deformation signal the general deformation pattern appears robust, especially since most deformations occur centred towards the cone, indicating that the displacement patterns are correctly captured. Assuming the reference point is stable, the background errors of the measured displacements are up to ~3 mm between interferograms (inferred from displacements within a 50 m window around the stable point). Despite this, additional ground control data (e.g. from GNSS monitoring stations) would be helpful to further increase the accuracies of deformation monitoring and reduce errors, although the high volcanic activity makes this a challenging and risky task.

Finally, as with most radar data, Sentinel-1 is not sensitive towards displacements in north and south directions. While there are likely significant motions of Anak Krakatau in these directions, these cannot be resolved accurately. We adapted our sandbox modelling approach to also focus mostly on vertical and east-west motion components, ensuring good comparability between our datasets.

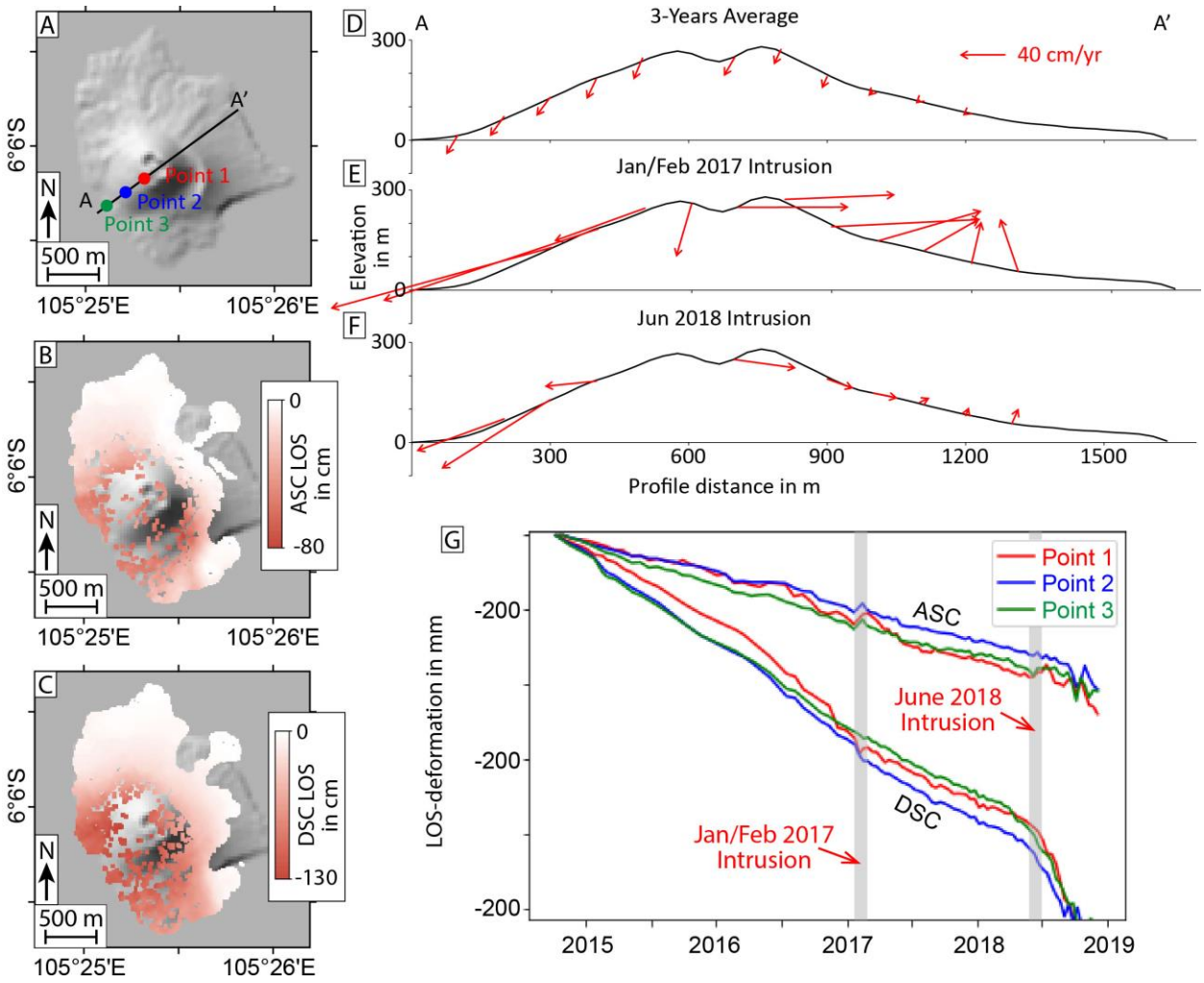


Figure S1: InSAR plots with profiles and selected points marked in A). The full flank motions in Line-of-Sight are shown for B) ascending and C) descending Orbits. The decomposed movement directions and rates as vectors on the Anak Krakatau surface for D) the 3-year average, E) the Jan/Feb 2017 intrusion, and F) the June 2018 intrusion (c.f. Fig. 2A-F). The deformation of the three selected points across the western flank, one near the summit, one in the mid-flank and one near the shore is shown in G). The LOS deformations are remarkably consistent throughout the entire flank, also showing the effects of the intrusions as deformation accelerations in DSC and decelerations in ASC, with the latter likely being the result of bulging, pushing the flank closer towards the satellite. However, the actual slip direction is still accelerated downwards as seen in the decomposed data shown in E) and F).

## SUPPLEMENT B: ANALOGUE SANDBOX MODELLING

### Experimental setup and results:

We study the interaction of décollement flank failure and magmatic intrusions by conducting analogue experiments using granular sand. For this purpose we reconstruct the Anak Krakatau with sand by building a simplified circular cone on a flat surface. We test the gradual sliding of the flank through a deep-seated basal décollement. Contrary to previous studies, we do not induce gravitational failure and décollement slip of the sand cone over a silicone layer (e.g. Merle and Borgia, 1996; Le Corvec and Walter, 2009; Byrne et al., 2013; Le Corvec et al., 2014), but create static experiment conditions by actively causing the slip through moving the basal décollement. This enables us to better compare the observed deformations of flank slip and intrusions, which naturally occur on different timescales and otherwise make non-static scaling challenging.

We conducted two types of deformation mechanisms for our sets of analogue experiments (Fig. S2), (1) the gradual sliding of the flank through a deep-seated basal décollement and (2) magma rise through a circular conduit using the setup and ~400 µm grain size sand used previously in Zorn et al. (2020) by intruding a sand column with a 4 cm diameter. We firstly perform these two deformation mechanisms separately (experiments A-B), then conduct another experiment starting with an initial décollement formation, followed by the column intrusion into the sand volcano with the previously destabilised flank (experiment C). All experiments were recorded with two DSLR-Cameras (Nikon D5100 and D7500) from a vertical (map) and horizontal (profile) viewing perspective, set to record in intervals between deformations (intervals depend on the mechanism). This enabled us to perform particle image velocimetry (PIV) to track the surface motions of the deforming sand cone, where we quantify pixel displacements between subsequent images. Here we used LaVision DaVis (version 10.0.5) to map the 2D displacement field of the sand cones in both viewing perspectives. For this purpose we employed decreasing sub-window squares with 256px side length and 128px side length (both with 75% overlap). This vector-based approach has the advantage that it can display the displacement field, but also calculate derivative deformation metrics such as strains and particle rotations (or vorticity), which can be used to visualise developing structures and faults. We additionally employ structure-from-motion photogrammetry with a handheld Camera (Pentax Ricoh GR) to further characterise morphological and volume changes in our models. For this purpose the sand-cones are photographed multiple times from different viewing angles in order to enable the reconstruction of a high resolution point cloud and

digital elevation model of the sand cones in sub-mm resolution. Here, Agisoft Metashape (version 1.8.0) was used to generate dense point clouds and orthomaps of the analogue volcanoes.

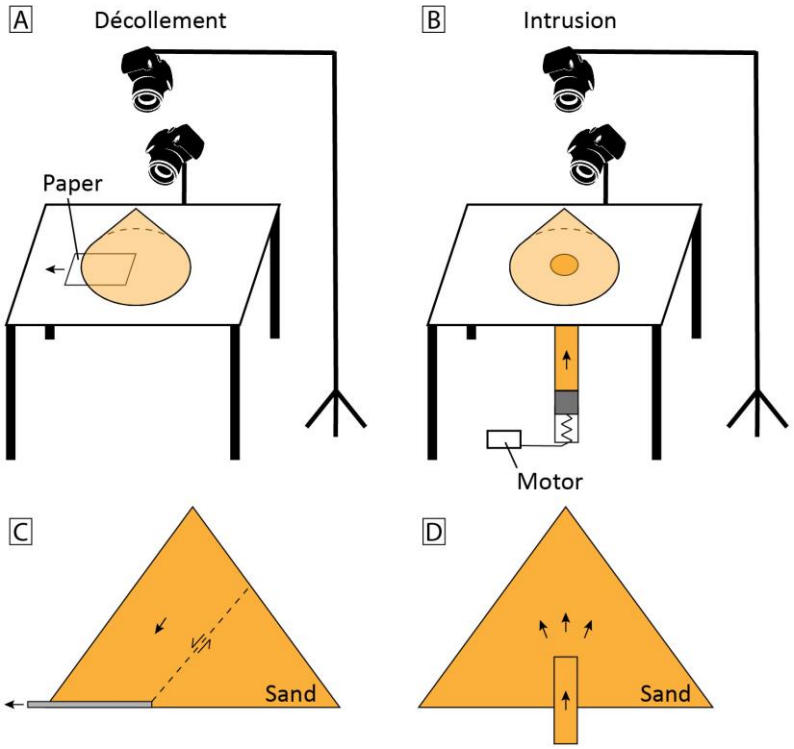


Fig. S2: Schematic setup drawing of the analogue experiment setup mechanisms and a profile view. A), C), décollement at the base of the sand volcano to induce flank sliding and B), D) circular intrusion of sand into the cone. B) is modified after Zorn et al. (2020).

In experiment A the flank deformations as a result of décollement slip were investigated (Fig. S3). For this purpose, we place a 210 mm wide (A4) paper sheet beneath one flank of the sand cone (starting 5 cm from the cone centre) that is moved outwards in small increments. As a result, the flank gradually destabilises and starts to slide outwards in two blocks separated by a set of steep antithetic faults (Fig. S3B-E). This is consistent with similar experiments incorporating artificial décollement slip in cones (Le Corvec and Walter, 2009). While the outer block moves laterally, the inner-block can be observed to move both down- and outwards. This includes the cone summit, reducing the overall height of the sand-volcano. Plotting the maximum normal strain in the vertical view, i.e. highlighting areas with particles moving apart or together, the faulting can be seen to affect the surface of the flank (Fig. S3C).

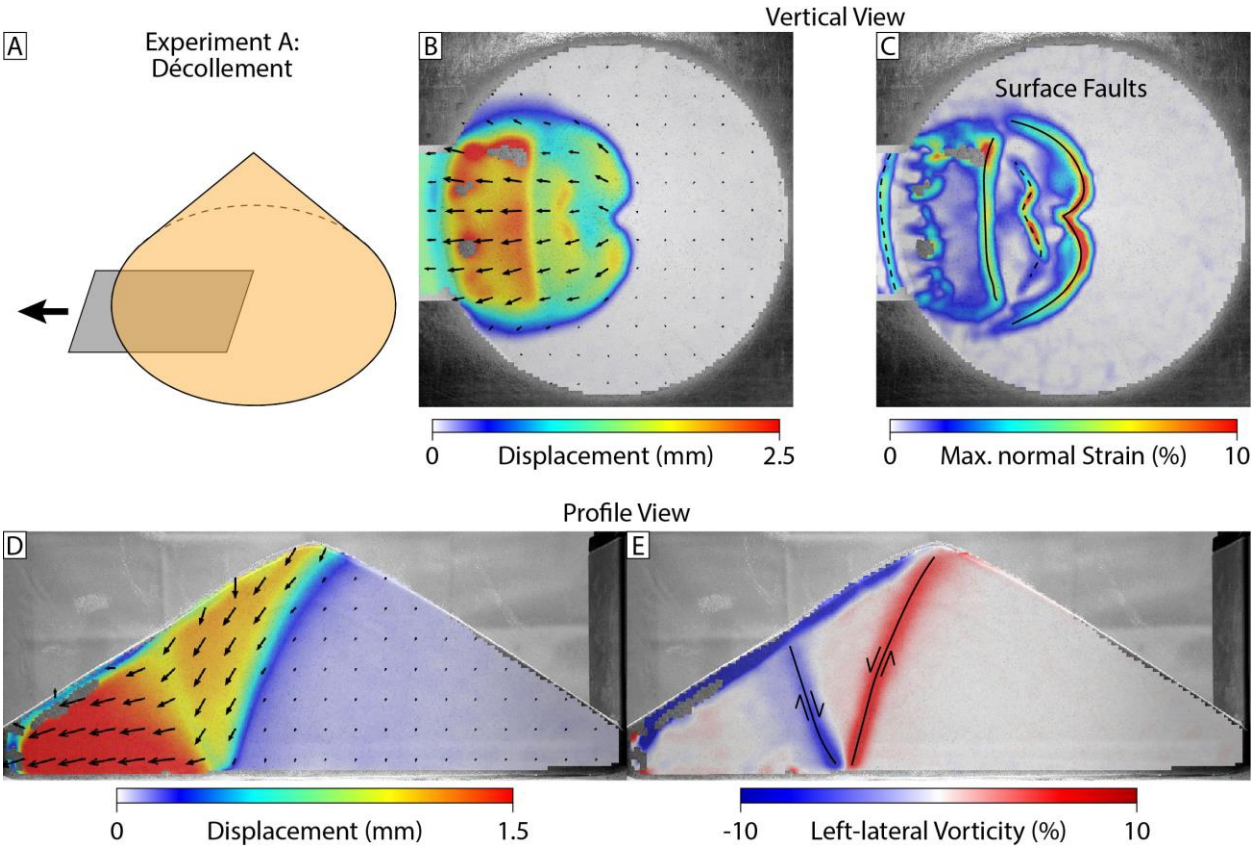


Fig. S3: Experiment A simulating the flank motion due to the décollement by moving a sheet of paper laterally underneath the cone. This is illustrated in A) and the particle image velocimetry results are shown in vertical view for the displacement field B) and maximum normal strain visualising surface faults C) as well as in profile view showing the displacement field D) and the vorticity, visualising shear faults and their direction E).

For experiment B we intruded a circular column of sand (4 cm diameter) into the centre of the sand cone without a pre-existing décollement (Fig. S4). Surprisingly, this did not result in uplift of the summit cone but rather its subsidence. This is caused by a set of inwards-dipping antithetic faults originating at the conduit (Fig. S4E), which are similar to the spine-bounding faults seen in Zorn et al. (2020). These redirect the vertical intrusion to laterally push the flanks outwards, in turn causing subsidence at the summit. As a result, the vertical change shows a height reduction in the cone centre and gain in the outer flanks (c.f. Fig. 2I, J). If the intrusion persists, it eventually channelizes the ascending magma along a curved set of faults towards the surface, forming a curved conduit through the cone (Fig. S4F, G). The direction of the curve appears to be random if the cone is circular and the intrusion centred (we confirmed this with repeat experiments), although

we cannot rule out that minor imbalance in these factors influenced the magma ascent direction. Similar previous experiments suggest the magma deflects towards the nearest slope, which is likely happening here as well (Acocella, 2005).

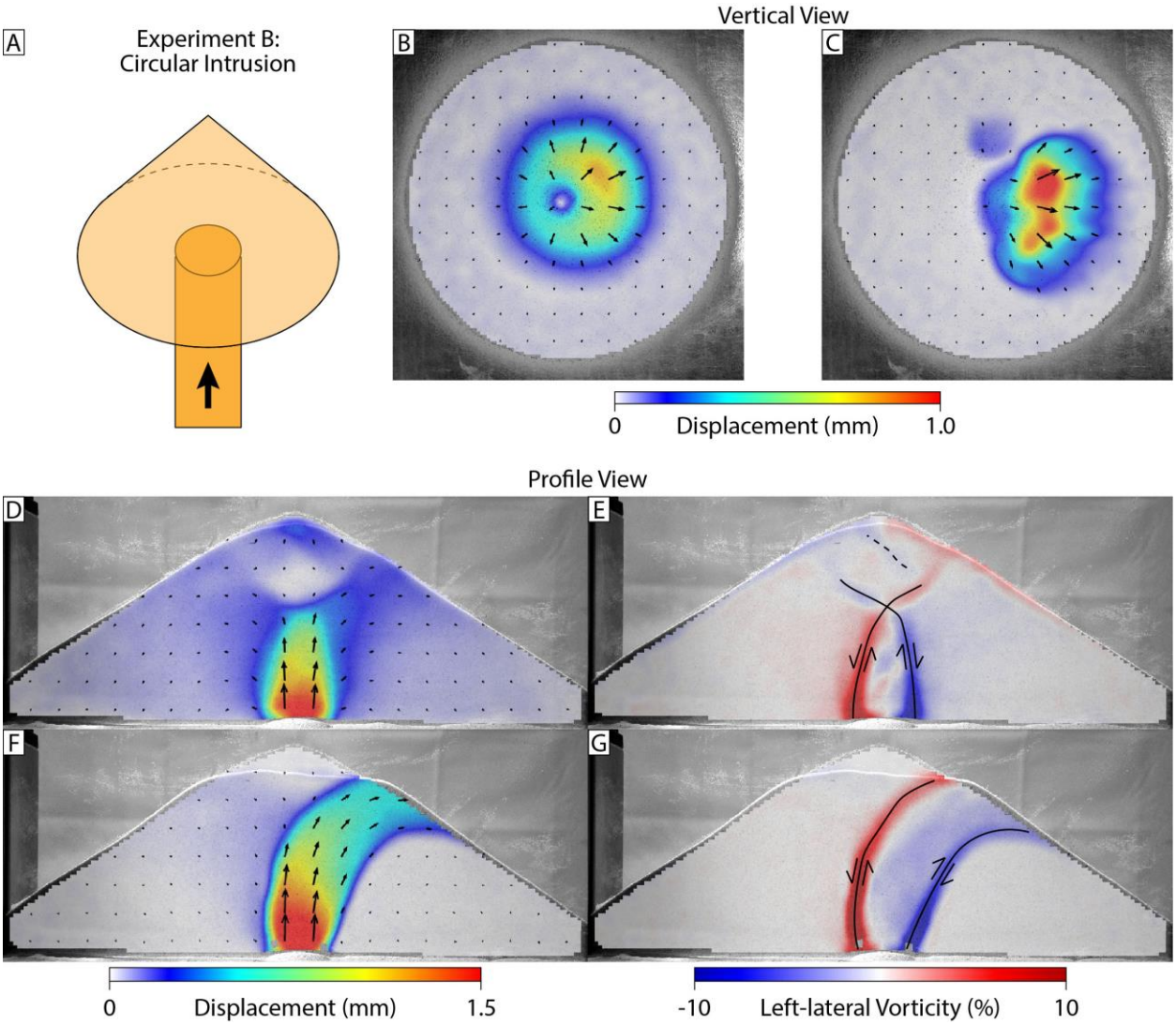


Fig. S4: Experiment B simulating a circular intrusion into the sand cone. This is illustrated in A) and the particle image velocimetry results are shown in vertical view for the displacement field in an early and late stage of the intrusion B), C) as well as in profile view showing the displacement field D), F) and the vorticity, visualising shear faults and their direction E), G) also at an early and late intrusion stage, respectively.

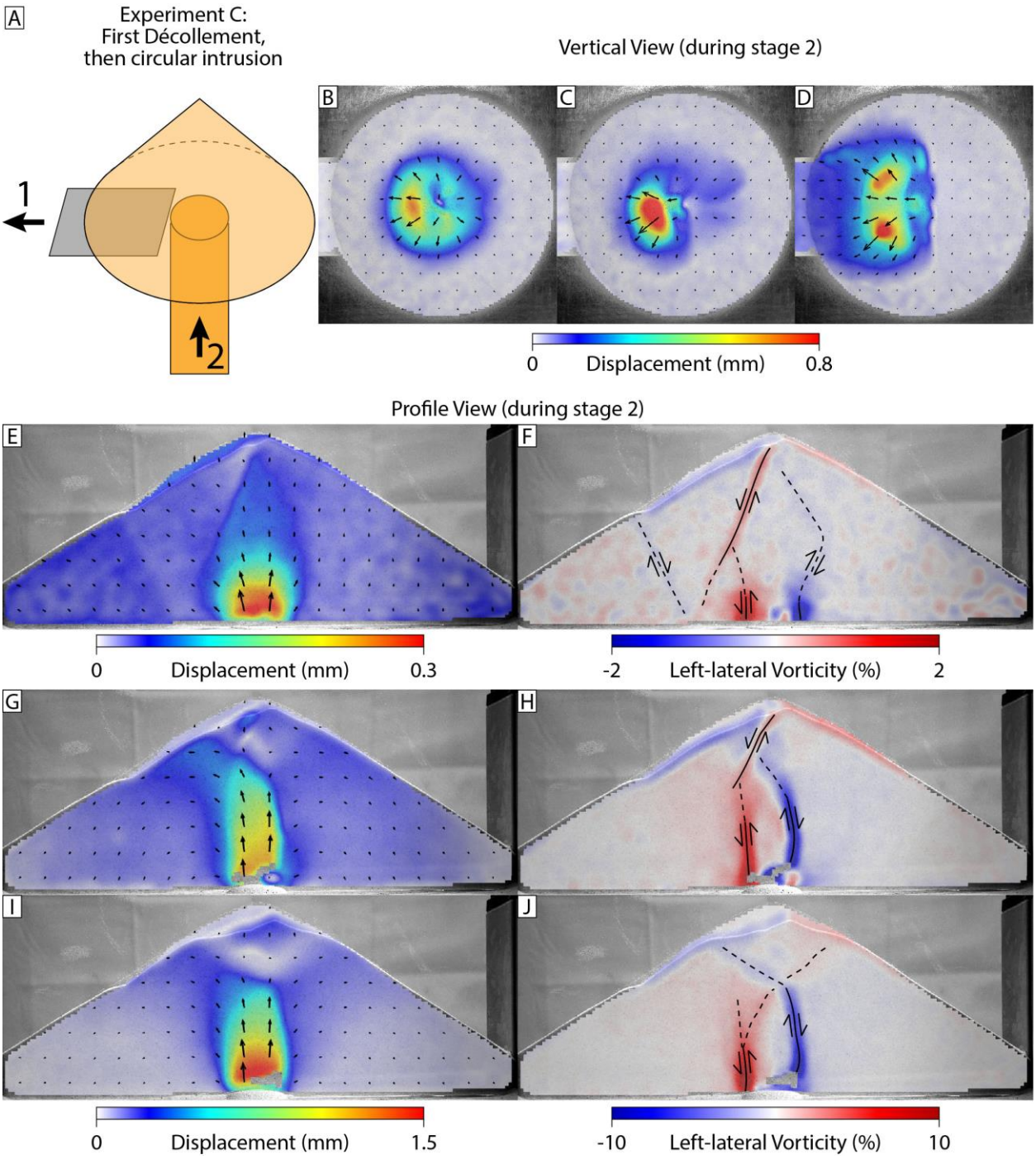


Fig. S5: Experiment C combines the décollement slip from experiments A (stage 1) and the circular intrusion from experiment B (stage 2). This is illustrated in A) and the particle image velocimetry results are shown in vertical view for the displacement field in an early and late stages of the intrusion B)-D) as well as in profile view showing the displacement field E), G), I) and the vorticity, visualising shear faults and their direction F), H), J) also at an early and late intrusion stage, respectively.

In experiment C, we combined the motions of experiments A and B, firstly forming a décollement, then intruding a circular sand column into the disturbed edifice (Fig. S5). This is also the experiment presented in the main paper (c.f. Fig. 3). The décollement is conducted identical to experiment A (Fig. S3), inducing the antithetic block faults into the sand cone. During the initial stages of the intrusion, we can observe a reactivation of the inner block fault, so the intrusion causes further flank slip even if the décollement is not moved anymore (Fig. S5E, F). After this and with continued intrusion, the same set of inwards-dipping faults form as in experiment B, gradually overprinting and slowing the flank slip (Fig S5G-J). In most cases, the magma then deflects towards the unstable flank (Fig. S5B-D, G-H), however, in repeat experiments we saw that it could also deflect towards the opposite side. In the later stages of the intrusion, the same motion dynamics as in experiment B are achieved, forming either a stable upwards intrusion or a curved conduit moving material towards the surface (Fig S5I-J).

**Materials and scaling:**

Considering that the flank of Anak Krakatau consists of largely unconsolidated pyroclastics (Decker and Hadikusumo, 1961; Grilli et al., 2019), we utilise dry low-cohesion rounded sand with ~400 μm grain sizes that was used to characterise lava dome and spine growth before with no added plaster powder (Rosenau et al., 2018; Zorn et al., 2020). The use of sand models is also static, meaning their deformations are rate-independent and their scaling can be simplified to consider only the geometry (Brothelande and Merle, 2015; Merle, 2015). Here we use the height/radius (H/R) ratio of the volcanic cone as a geometrical orientation. Using a digital elevation model, here the freely available Copernicus DEM GLO-30 (Airbus, 2020), we measure an approximate cone height of 290 m and an approximate 600 m basal radius (assuming a simplified circular cone) for Anak Krakatau. This means an H/R-Ratio of 0.48 for the real volcano, equalling a ~26° slope angle. We find that our sand models produce a similar, but slightly steeper topography with a consistent H/R-Ratio of 0.58 and a ~30° slope angle. Thus, our experiments can be expected to behave dynamically similar to a real volcanic cone, however, it should be noted that the edifice was not unstable on its own, meaning that our models cannot explain the initial formation of the décollement and required artificial activation. This also prevents a meaningful scaling and quantitative assessment of the frictional sliding process and limits the outcomes to the observation of deformation patterns and the structural architecture of the cone.

A further point to consider is the suitability of unconsolidated sand as an analogue material for the volcanic cone and the intruding magma. Such material is commonly used for crustal analogue models (often in combination with flour or plaster powder to vary cohesion) (Galland et al., 2009; Poppe et al., 2021) and here pure sand thus has suitable properties to model the very low cohesion and unconsolidated pyroclastic deposits of Anak Krakatau's SW-Flank. However, it is not clear how well it represents the crustal elastic properties (Poppe et al., 2019), likely comprising the bulk of the Anak Krakataus edifice, however, they do exert elastic deformation and strain hardening before brittle plastic failure (Lohrmann et al., 2003; Panien et al., 2006). Consequently, many modelled deformations should be suitable for a comparison with InSAR-data, which is assumed to measure brittle-elastic ground deformations.

Assessing the suitability of the magma analogue is more challenging, since sand cannot represent viscous properties well. Many other studies have successfully used and scaled viscous material such as silicone oil or golden syrup for testing magmatic intrusions into volcanic edifices (Donnadieu and Merle, 1998; Merle and Donnadieu, 1999; Kervyn et al., 2009; Poppe et al., 2019). As we present two-stage deformation experiments with different processes acting on different and unclear timescales, we instead use simplified static models using only non-viscous sand. Thus, we are limited to semi-brittle lava dome style intrusions (Zorn et al., 2020), but the resulting stress field and displacement are likely to behave very similarly considering their purpose of overlying ground deformation and structure activation. In particular, this applies to the distributed stress induced by our conduit intrusion causing shear faulting. It is known that a mixed mode of opening and shear fracturing is expected for low cohesion material even with viscous material such as golden syrup (Poppe et al., 2019). In terms of the intrusion geometry, these properties also lead to cup-shaped intrusions and cryptodomes rather than dykes, which are more typical for higher-cohesion crustal analogues (Poppe et al., 2019). Despite these differences, we find that our results agree well with previous scaled experiments using viscous intrusions. In particular, the general pattern of summit subsidence and outwards flank bulging is found in most similar experiments and the inwards dipping shear faults from the conduit (Fig. S4E) are comparable to a more rigid indenter intrusion (Merle and Donnadieu, 1999), which is reasonable considering the brittle material.

**Modelling Limitations:**

Analogue models and experiments always require simplifications in order to understand the main acting processes, so not all complexities in a real volcano can be considered. Most notably for our experiments, the dimensions, shape and location of the intrusions are somewhat speculative. While InSAR is capable of inferring such metrics from surface deformation by means of modelling, e.g. by utilising Mogi sources (e.g. Baker and Amelung, 2012), these are typically rather complex when they are in very shallow environments (Salzer et al., 2014). Due to the small size of Anak Krakau and the partial obscuration of flank deformations by the sea this is not trivial and the varying coherences, particularly from June 2018 onwards after activity increased, further complicate this. Here, we observe a generally very good agreement of our modelled deformation patterns, using a uniform circular intrusion, with the observed ones by InSAR (Fig. 2), however, the exact shape and magnitude of our intrusions should still be seen with some caution. Furthermore, structural features and material heterogeneities present in the lithology of the island are neglected as we use homogeneous dry sand. The slightly older eastern part of the island likely has other ground and rock properties than the newly built flank consisting of young pyroclastic deposits and lavas that were built up very rapidly by the growing volcanic island. Since we mainly aim at simulating deformations on the flank, where consolidation times are low, we use very low cohesion sand without plaster powder. This approach is likely appropriate, but may not properly reflect the behaviour of older island deposits, which are likely denser and more resistant to deformation. Interactions of the unstable flank with seawater can also not be considered here, although this is a potentially relevant factor as the collapse occurred partially underwater. In particular, hydrothermal alteration associated with increased fluid circulation due to the exposure of seawater can be expected to impact edifice stability and increase deformations (e.g. Heap et al., 2021), however, such interactions are notoriously complex and cannot be considered by our models.

Another important aspect considering the model limitations is the simplified deformation mechanisms. For the décollement, we use a horizontal sliding plane, which is generally realistic at other volcanoes (Denlinger and Okubo, 1995; De Vries and Borgia, 1996), however, it is not clear whether this particular orientation exists at Anak Krakatau. Most studies consider a sub-horizontal sliding plane that steepens towards the cone, which would be consistent with the main fault forming in our experiments (Fig. S3E), however, these are typically known for large basaltic volcanoes such as Kilauea and Mauna Loa (Hawaii), or Etna (Italy) (Denlinger and Okubo, 1995;

Lundgren et al., 2004; Walter and Amelung, 2006). Here, we could not test how deformations would differ to an inclined décollement, which may have reduced the outer block rise (Fig. 2G), but find the developing steep main fault consistent with field and other modelling data (Acocella, 2005; Le Corvec et al., 2014; Hunt et al., 2021). We also actively induce the destabilisation as we pull on the paper representing the sliding plane, which is different to the natural process. At Anak Krakatau, gravitational instability mixed with the structural architecture of the cone and caldera causing the gradual sliding are considered to be the most likely explanation (Hunt et al., 2021; Cutler et al., 2022). This also prevents any quantitative assessments inferring the stresses, pressures, or strains acting on the faults using the scaled models as the underlying processes are not the same, however, the resulting structural architecture is likely comparable. For the intrusion mechanisms, the circular sand column is a strongly simplified magma emplacement analogue and limited in size and extent, making controlled scaling only possible by varying the size of the overlying sand cone. The circular intrusion injects magma similar to a dome extrusion, which is what this setup was originally designed for (Zorn et al., 2020). However, since there is a full sand cone and thus a confining edifice above the intrusion, the initial deformations are different to dome extrusions, causing an upwards spreading motion due to the pressure of the intruding material. Thus, the experiments may be appropriate to simulate initial shallow pressurisation in volcanic edifices, which is why our results match the observed InSAR data well, but if the intrusions persist for long the new material will eventually surface and start a dome extrusion (Fig. S4F, G). This has actually been observed at Anak Krakatau in Oct 2018 and gives us some confidence in this method (Hochfeld et al., 2022).

## SUPPLEMENT C: THERMAL EMISSIONS OF ANAK KRAKATAU

Thermal activity recorded by satellite data captures peaks in the volcano's radiative power (VRP) during strombolian or vulcanian eruption activity. MODIS data presented here was elaborated by the MIROVA system (Coppola et al., 2016) and published in Walter et al. (2019). This data indicates eruptive phases at Anak Krakatau for the past 20 years visible as spikes in the VRP, showing at least 10 intense periods in 2000-2001, in 2007-2009, in 2010-2012 and in 2017-2018 (Fig. S6). Deformations of the SW Flank of Anak Krakatau were detected by Chaussard and Amelung (2012) in 2006-2009 and by this study in 2014-2018. Since the two eruptions in 2017 and 2018 also caused flank slip accelerations, it is likely that similar instances also occurred during past eruptions at this volcano. The two eruptions and VRP spikes also coincide with the detected intrusion events (c.f. Fig. 1C), further supporting the interpretation of arriving new magma during these times.

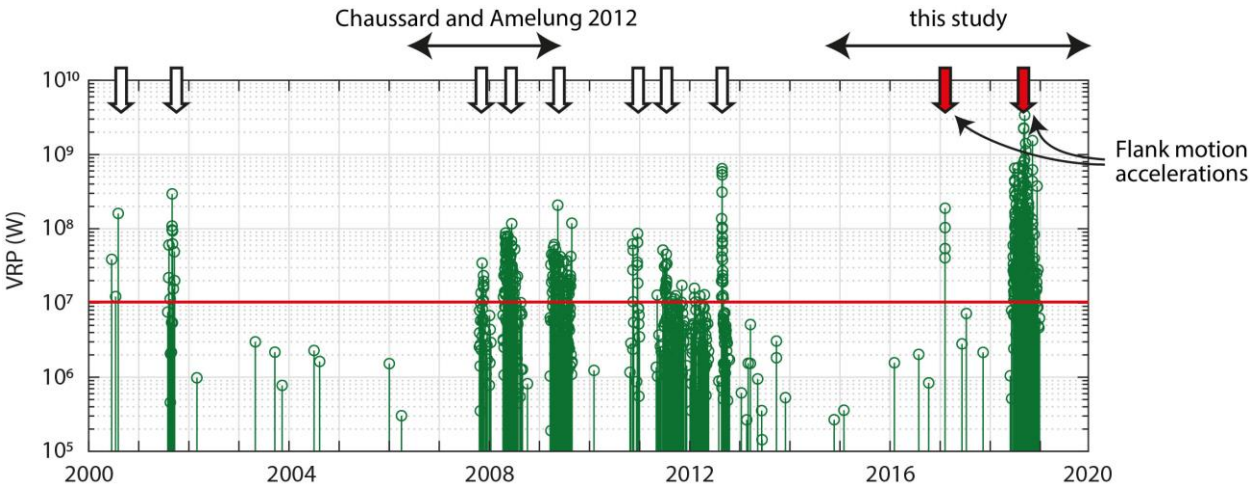


Fig. S6: Volcanic Radiative Power (VRP) of Anak Krakatau between 2000 and 2019 modified after Walter et al. (2019). The arbitrary red line at $10^7$ W indicates the apparent threshold for significant events, resulting in at least 10 distinct episodes of volcanic activity during this time. The InSAR observation periods of this study and Chaussard and Amelung (2012) are also shown.

**SUPPLEMENT REFERENCES:**


Acocella, V., 2005. Modes of sector collapse of volcanic cones: Insights from analogue experiments. Journal of Geophysical Research: Solid Earth, 110(B2). DOI: 10.1029/2004JB003166

Airbus, 2020. Copernicus DEM Validation Report (v2.1), https://spacedata.copernicus.eu/documents/20126/0/GEO1988-CopernicusDEM-SPE-002_ProductHandbook_I1.00.pdf.

Baker, S. and Amelung, F., 2012. Top-down inflation and deflation at the summit of Kīlauea Volcano, Hawai'i observed with InSAR. Journal of Geophysical Research: Solid Earth, 117(B12). DOI: 10.1029/2011JB009123

Berardino, P., Fornaro, G., Lanari, R. and Sansosti, E., 2002. A new algorithm for surface deformation monitoring based on small baseline differential SAR interferograms. IEEE Transactions on Geoscience and Remote Sensing, 40(11): 2375-2383. DOI: 10.1109/TGRS.2002.803792

Brothelande, E. and Merle, O., 2015. Estimation of magma depth for resurgent domes: An experimental approach. Earth and Planetary Science Letters, 412: 143-151. DOI: 10.1016/j.epsl.2014.12.011

Byrne, P.K., Holohan, E.P., Kervyn, M., van Wyk de Vries, B., Troll, V.R. and Murray, J.B., 2013. A sagging-spreading continuum of large volcano structure. Geology, 41(3): 339-342. DOI: 10.1130/g33990.1

Chaussard, E. and Amelung, F., 2012. Precursory inflation of shallow magma reservoirs at west Sunda volcanoes detected by InSAR. Geophysical Research Letters, 39(21). DOI: 10.1029/2012GL053817

Coppola, D., Laiolo, M., Cigolini, C., Donne, D.D. and Ripepe, M., 2016. Enhanced volcanic hot-spot detection using MODIS IR data: results from the MIROVA system. Geological Society, London, Special Publications, 426(1): 181-205. DOI: doi:10.1144/SP426.5

Cutler, K.S., Watt, S.F.L., Cassidy, M., Madden-Nadeau, A.L., Engwell, S.L., Abdurrachman, M., Nurshal, M.E.M., Tappin, D.R., Carey, S.N., Novellino, A., Hayer, C., Hunt, J.E., Day, S.J., Grilli, S.T., Kurniawan, I.A. and Kartadinata, N., 2022. Downward-propagating eruption following vent unloading implies no direct magmatic trigger for the 2018 lateral collapse of Anak Krakatau. Earth and Planetary Science Letters, 578: 117332. DOI: 10.1016/j.epsl.2021.117332

De Vries, B.V.W. and Borgia, A., 1996. The role of basement in volcano deformation. Geological Society, London, Special Publications, 110(1): 95. DOI: 10.1144/GSL.SP.1996.110.01.07

Decker, R.W. and Hadikusumo, D., 1961. Results of the 1960 expedition to Krakatau. Journal of Geophysical Research (1896-1977), 66(10): 3497-3511. DOI: 10.1029/JZ066i010p03497

Denlinger, R.P. and Okubo, P., 1995. Structure of the mobile south flank of Kilauea Volcano, Hawaii. Journal of Geophysical Research: Solid Earth, 100(B12): 24499-24507. DOI: 10.1029/95JB01479

Donnadieu, F. and Merle, O., 1998. Experiments on the indentation process during cryptodome intrusions: New insights into Mount St. Helens deformation. Geology, 26(1): 79-82. DOI: 10.1130/0091-7613(1998)026<0079:EOTIPD>2.3.CO;2

Galland, O., Planke, S., Neumann, E.R. and Malthe-Sørenssen, A., 2009. Experimental modelling of shallow magma emplacement: Application to saucer-shaped intrusions. Earth and Planetary Science Letters, 277(3): 373-383. DOI: 10.1016/j.epsl.2008.11.003

Goldstein, R.M. and Werner, C.L., 1998. Radar interferogram filtering for geophysical applications. Geophysical Research Letters, 25(21): 4035-4038. DOI: 10.1029/1998GL900033

Grilli, S.T., Tappin, D.R., Carey, S., Watt, S.F.L., Ward, S.N., Grilli, A.R., Engwell, S.L., Zhang, C., Kirby, J.T., Schambach, L. and Muin, M., 2019. Modelling of the tsunami from the December 22, 2018 lateral collapse of Anak Krakatau volcano in the Sunda Straits, Indonesia. Scientific Reports, 9(1): 11946. DOI: 10.1038/s41598-019-48327-6

Heap, M.J., Baumann, T., Gilg, H.A., Kolzenburg, S., Ryan, A.G., Villeneuve, M., Russell, J.K., Kennedy, L.A., Rosas-Carbajal, M. and Clynne, M.A., 2021. Hydrothermal alteration can result in pore pressurization and volcano instability. Geology, 49(11): 1348-1352. DOI: 10.1130/G49063.1

Hochfeld, I., Hort, M., Schwalbe, E. and Dürig, T., 2022. Eruption dynamics of Anak Krakatau volcano (Indonesia) estimated using photogrammetric methods. Bulletin of Volcanology, 84(8): 73. DOI: 10.1007/s00445-022-01579-z

Hunt, J.E., Tappin, D.R., Watt, S.F.L., Susilohadi, S., Novellino, A., Ebmeier, S.K., Cassidy, M., Engwell, S.L., Grilli, S.T., Hanif, M., Priyanto, W.S., Clare, M.A., Abdurrachman, M. and Udrekh, U., 2021. Submarine landslide megablocks show half of Anak Krakatau island failed on December 22nd, 2018. Nature Communications, 12(1): 2827. DOI: 10.1038/s41467-021-22610-5

Kervyn, M., Ernst, G.G.J., van Wyk de Vries, B., Mathieu, L. and Jacobs, P., 2009. Volcano load control on dyke propagation and vent distribution: Insights from analogue modeling. Journal of Geophysical Research: Solid Earth, 114(B3). DOI: 10.1029/2008JB005653

Le Corvec, N. and Walter, T.R., 2009. Volcano spreading and fault interaction influenced by rift zone intrusions: Insights from analogue experiments analyzed with digital image correlation technique. Journal of Volcanology and Geothermal Research, 183(3): 170-182. DOI: 10.1016/j.jvolgeores.2009.02.006

Le Corvec, N., Walter, T.R., Ruch, J., Bonforte, A. and Puglisi, G., 2014. Experimental study of the interplay between magmatic rift intrusion and flank instability with application to the 2001 Mount Etna eruption. Journal of Geophysical Research: Solid Earth, 119(7): 5356-5368. DOI: 10.1002/2014jb011224

Lohrmann, J., Kukowski, N., Adam, J. and Oncken, O., 2003. The impact of analogue material properties on the geometry, kinematics, and dynamics of convergent sand wedges. Journal of Structural Geology, 25(10): 1691-1711. DOI: 10.1016/S0191-8141(03)00005-1

Lundgren, P., Casu, F., Manzo, M., Pepe, A., Berardino, P., Sansosti, E. and Lanari, R., 2004. Gravity and magma induced spreading of Mount Etna volcano revealed by satellite radar interferometry. Geophysical Research Letters, 31(4). DOI: 10.1029/2003GL018736

Merle, O. and Borgia, A., 1996. Scaled experiments of volcanic spreading. Journal of Geophysical Research: Solid Earth, 101(B6): 13805-13817. DOI: 10.1029/95JB03736

Merle, O. and Donnadieu, F., 1999. Indentation of volcanic edifices by the ascending magma. Geological Society, London, Special Publications, 174(1): 43-53. DOI: doi:10.1144/GSL.SP.1999.174.01.03

Merle, O., 2015. The scaling of experiments on volcanic systems. Frontiers in Earth Science, 3(26): 1-14. DOI: 10.3389/feart.2015.00026

Panien, M., Schreurs, G. and Pfiffner, A., 2006. Mechanical behaviour of granular materials used in analogue modelling: insights from grain characterisation, ring-shear tests and analogue

experiments. Journal of Structural Geology, 28(9): 1710-1724. DOI: 10.1016/j.jsg.2006.05.004

Pepe, A. and Calò, F., 2017. A Review of Interferometric Synthetic Aperture RADAR (InSAR) Multi-Track Approaches for the Retrieval of Earth's Surface Displacements. Applied Sciences, 7(12): 1264. DOI: 10.3390/app7121264

Poppe, S., Holohan, E.P., Galland, O., Buls, N., Van Gompel, G., Keelson, B., Tournigand, P.Y., Brancart, J., Hollis, D., Nila, A. and Kervyn, M., 2019. An Inside Perspective on Magma Intrusion: Quantifying 3D Displacement and Strain in Laboratory Experiments by Dynamic X-Ray Computed Tomography. Frontiers in Earth Science, 7. DOI: 10.3389/feart.2019.00062

Poppe, S., Holohan, E.P., Rudolf, M., Rosenau, M., Galland, O., Delcamp, A. and Kervyn, M., 2021. Mechanical properties of quartz sand and gypsum powder (plaster) mixtures: Implications for laboratory model analogues for the Earth's upper crust. Tectonophysics, 814: 228976. DOI: 10.1016/j.tecto.2021.228976

Rosenau, M., Pohlenz, A., Kemnitz, H. and Warsitzka, M., 2018. Ring-shear test data of quartz sand G12 used for analogue experiments in the Helmholtz Laboratory for Tectonic Modelling (HelTec) at the GFZ German Research Centre for Geosciences in Potsdam. GFZ Data Services, 10.5880/GFZ.4.1.2019.003. DOI: 10.5880/GFZ.4.1.2019.003

Salzer, J.T., Nikkhoo, M., Walter, T.R., Sudhaus, H., Reyes-Dávila, G., Bretón, M. and Arámbula, R., 2014. Satellite radar data reveal short-term pre-explosive displacements and a complex conduit system at Volcán de Colima, Mexico. Frontiers in Earth Science, 2(12): 1-11. DOI: 10.3389/feart.2014.00012

Walter, T.R. and Amelung, F., 2006. Volcano-earthquake interaction at Mauna Loa volcano, Hawaii. Journal of Geophysical Research: Solid Earth, 111(B5). DOI: 10.1029/2005JB003861

Walter, T.R., Haghshenas Haghighi, M., Schneider, F.M., Coppola, D., Motagh, M., Saul, J., Babeyko, A., Dahm, T., Troll, V.R., Tilmann, F., Heimann, S., Valade, S., Triyono, R., Khomarudin, R., Kartadinata, N., Laiolo, M., Massimetti, F. and Gaebler, P., 2019. Complex hazard cascade culminating in the Anak Krakatau sector collapse. Nature Communications, 10(1): 4339. DOI: 10.1038/s41467-019-12284-5

Yun, S., Segall, P. and Zebker, H., 2006. Constraints on magma chamber geometry at Sierra Negra Volcano, Galápagos Islands, based on InSAR observations. Journal of Volcanology and Geothermal Research, 150(1): 232-243. DOI: 10.1016/j.jvolgeores.2005.07.009

Zorn, E.U., Walter, T.R., Heap, M.J. and Kueppers, U., 2020. Insights into lava dome and spine extrusion using analogue sandbox experiments. Earth and Planetary Science Letters, 551: 116571. DOI: 10.1016/j.epsl.2020.116571